PROCEEDINGS OF SPIE

SPIEDigitalLibrary.org/conference-proceedings-of-spie

Deformable registration of histological cancer margins to gross hyperspectral images using demons

Martin Halicek, James V. Little, Xu Wang, Zhuo Georgia Chen, Mihir Patel, et al.

Martin Halicek, James V. Little, Xu Wang, Zhuo Georgia Chen, Mihir Patel, Christopher C. Griffith, Mark W. El-Deiry, Nabil F. Saba, Amy Y. Chen, Baowei Fei, "Deformable registration of histological cancer margins to gross hyperspectral images using demons," Proc. SPIE 10581, Medical Imaging 2018: Digital Pathology, 105810N (6 March 2018); doi: 10.1117/12.2293165

SPIE.

Event: SPIE Medical Imaging, 2018, Houston, Texas, United States

Deformable Registration of Histological Cancer Margins to Gross Hyperspectral Images using Demons

Martin Halicek[a,b], James V. Little[c], Xu Wang[d], Zhuo Georgia Chen[d], Mihir Patel[e,f], Christopher C. Griffith[c], Mark W. El-Deiry[e,f], Nabil F. Saba[d], Amy Y. Chen[e,f], and Baowei Fei[a,f,g,h]

[a]Georgia Institute of Technology & Emory University, Wallace H. Coulter Department of Biomedical Engineering, Atlanta, GA, USA
[b]Medical College of Georgia, Augusta University, Augusta, GA, USA
[c]Emory University School of Medicine, Department of Pathology and Laboratory Medicine, Atlanta, GA, USA
[d]Emory University School of Medicine, Department of Hematology and Medical Oncology, Atlanta, GA, USA
[e]Emory University School of Medicine, Department of Otolaryngology, Atlanta, GA, USA
[f]Winship Cancer Institute of Emory University, Atlanta, GA, USA
[g]Emory University, Department of Mathematics and Computer Science, Atlanta, GA, USA
[h]Emory University, Department of Radiology and Imaging Sciences, Atlanta, GA, USA

ABSTRACT

Hyperspectral imaging (HSI), a non-contact optical imaging technique, has been recently used along with machine learning technique to provide diagnostic information about *ex-vivo* surgical specimens for optical biopsy. The computer-aided diagnostic approach requires accurate ground truths for both training and validation. This study details a processing pipeline for registering the cancer-normal margin from a digitized histological image to the gross-level HSI of a tissue specimen. Our work incorporates an initial affine and control-point registration followed by a deformable Demons-based registration of the moving mask obtained from the histological image to the fixed mask made from the HS image. To assess registration quality, Dice similarity coefficient (DSC) measures the image overlap, visual inspection is used to evaluate the margin, and average target registration error (TRE) of needle-bored holes measures the registration error between the histologic and HSI images. Excised tissue samples from seventeen patients, 11 head and neck squamous cell carcinoma (HNSCCa) and 6 thyroid carcinoma, were registered according to the proposed method. Three registered specimens are illustrated in this paper, which demonstrate the efficacy of the registration workflow. Further work is required to apply the technique to more patient data and investigate the ability of this procedure to produce suitable gold standards for machine learning validation.

Keywords: Hyperspectral imaging, digital histology, Demons registration, head and neck cancer surgery

1. INTRODUCTION

Head and neck cancer encompasses malignant neoplasms of the oral cavity, nasal cavity, pharynx, and larynx. Significant risk factors for the development of these types of cancer are tobacco consumption, alcohol consumption, and exposure to human papillomavirus (HPV).[1] Moreover, squamous cell carcinoma (SCCa) represents approximately 90% of cancer at these sites.[2] These cancers account for approximately 350,000 cancer deaths per year, and approximately 650,000 patient will be diagnosed with head and neck cancer each year.[1] Initial diagnosis includes patient examination, biopsy with histopathology, and imaging with CT, MRI, or PET to

Further author information: (Send correspondence to B.F.)
B.F.: e-mail: bfei@emory.edu website: fei-lab.org

Medical Imaging 2018: Digital Pathology, edited by John E. Tomaszewski, Metin N. Gurcan,
Proc. of SPIE Vol. 10581, 105810N · © 2018 SPIE · CCC code:
1605-7422/18/$18 · doi: 10.1117/12.2293165

determine staging of the disease. Additionally, a standard treatment is surgical cancer resection by a head and neck surgeon.

The most common practice during surgery to identify cancer margins is frozen section analysis, which can take 20 to 45 minutes.[3–5] When determining negative and positive cancer margins, most studies on oral cavity and aerodigestive tract cancers typically use a threshold of normal tissue beyond the tumor site greater than 5 mm to define margin adequacy.[4] Studies comparing disease recurrence using the 5 mm margin definition found that locoregional recurrence rates for inadequate versus adequate margins range from 30-55% for positive margins compared to only 12-18% for negative margins.[6–8] Moreover, disease recurrence greatly affects likelihood for additional surgeries, reduced quality of life, and increased mortality rates.[9] Five studies, comprising 1,200 patients, found that positive cancer margins have a greatly reduced disease survival, ranging from 7-52%, compared to disease-free survival rates of 39-73% for negative margins.[6–8,10,11]

Computer-aided diagnostic systems can be trained and optimized on confirmed examples of normal and cancer specimens to create a classification predictions on new patient data. The meaningfulness and generalizability of the reported performance of a system is dependent on the validity of the confirmed diagnoses.[12] Hyperspectral imaging (HSI) is a non-contact optical imaging technique, recently used along with machine learning and artificial intelligence algorithms to provide diagnostic information about *ex-vivo* surgical specimens. However, a consistent, reliable, and reproducible technique for ground-truth cancer margin delineation is needed for validation of HSI-based classifiers. This study aims to develop a processing pipeline for deformable registration of the histological cancer margin to HSI of *ex-vivo* tissue samples for future use as validation for a classifier. This technique is necessary to further investigate the potential of HSI for cancer detection.

2. METHODS

2.1 Experimental Design

In collaboration with Otolaryngology Department and the Department of Pathology and Laboratory Medicine at Emory University Hospital Midtown, head and neck cancer patients scheduled for surgical cancer resection were recruited for our study to create a database of HSI of *ex-vivo* tissue samples. Informed consent was obtained from all patients in accordance with Emory Institutional Review Board policies under the Head and Neck Satellite Tissue Bank protocol. Eleven patients with head and neck squamous cell carcinoma (HNSCCa) of the aerodigestive tract and six patients with thyroid carcinoma were included in this study. A schematic of the experimental design is shown in Figure 1. From each patient, three tissue samples approximately $10 \times 10 \times 3$ mm were collected: a sample of the tumor, a normal tissue sample, and a sample at the tumor-normal interface.[13–15] The collected tissues were kept in cold $1\times$ phosphate buffered solution during transport to the imaging laboratory at Emory University where the specimens were imaged. After HS imaging, samples are fixed in formalin and sectioned to create corresponding histological gold standards.

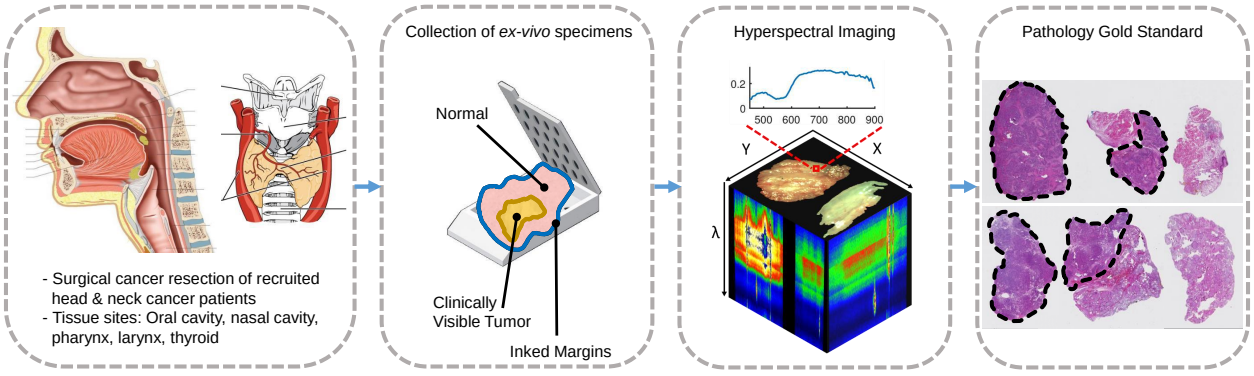

Figure 1. Flowchart of the hyperspectral imaging experiment on surgical tissue specimens.

Figure 2. Flowchart of the proposed method for registration of histological cancer margins to HSI.

2.2 Hyperspectral Imaging

Tissues were placed on an imaging board to acquire the hyperspectral imaging cube (hypercube). Additionally, a few tissue specimens were bored with a needle to make holes for target registration error analysis. The hyperspectral images were acquired using a CRI imaging system (Perkin Elmer Inc., Waltham, MA, USA), which is comprised of a Xenon white-light illumination source, a liquid crystal tunable filter, and a 16-bit charge-coupled device capturing images at a resolution of 1,040 by 1,392 pixels and a spatial resolution of 25 μm per pixel.[14–16] The hypercube contains 91 spectral bands, ranging from 450 to 900 nm at a 5 nm spectral sampling frequency. RGB composite images were created from each hypercube for use in registration.

2.3 Histopathology

After HSI, the tissue samples are inked to preserve orientation and placed in formalin. The specimens are then paraffin embedded, sectioned, hematoxylin and eosin stained, and digitized. A specialized head and neck cancer pathologist determines the composition of each tissue specimen and outlines the cancer margin of tissue samples containing an interface between cancer and normal tissue using Aperio ImageScope (Leica Biosystems Inc, Buffalo Grove, IL, USA).

2.4 Deformable Registration Pipeline

A binary mask is created from the HSI RGB composite image. A binary mask is also created from the histological image. These two binary masks are used as the input of the registration algorithm that was implemented with MATLAB (MathWorks Inc, Natick, MA, USA). A flowchart of the proposed registration method is shown in Figure 2. For samples with needle-bored holes, the average target registration error (TRE) was calculated from the center of the needle-bored hole after registration.[17] An affine registration is performed using rotation, translation, and scale to produce a non-reflective similarity transformation.[18] This step is necessary to get the histology mask approximately aligned to the neighborhood of the HSI mask. If the affine registration is not sufficient by visual inspection, an optional control-point registration is applied using control point pairs selected from the tissue edges of the masks. The control point registration is implemented by a local weighted mean of inferred second degree polynomials from each neighboring control point pair to create a transformation mapping.[19,20]

Demons registration is based on an analogy to Maxwell's Demons, in which every pixel in an image is an effector with a force, referred to as a demon, in total used to create a deformation field. A free-form deformation is made from the individual displacements of the complete grid of effectors (demons) in an image, and a Gaussian filter is applied to smooth the image and to create a regular displacement field.[21] The displacement field is determined by points scattered along the contours of binary masks. This process is performed iteratively, and the displacement of each effector at each iteration is calculated using optical flow, which represents small displacements derived from diffusion model behavior.[21,22]

The Demons registration method was applied in the deformable registration pipeline. After the affine and control-point based registration, the transformed histology mask is registered to the HSI mask using deformable Demons registration with an accumulated field smoothing value of 0.5 for five pyramid levels with one thousand iterations per pyramid level.[21]

To evaluate the efficacy of the proposed registration methods, 17 tissue samples from 11 HNSCCa and 6 thyroid cancer patients were registered. Dice similarity coefficient (DSC) was calculated by measuring the overlap of the histological and HSI mask. Target registration error (TRE) was calculated using both needle-bored holes in samples when available and tissue landmarks visible between gross and histology to obtain an average Euclidean distance representing error.[20] The TRE and DSC were calculated for each tissue sample, and averages were obtained for both groups.

Table 1. Targeted registration error (TRE) and Dice similarity coefficient (DSC) for the registration between hyperspectral images and digitized histological images.

Group	Registration Method	TRE (mm)	DSC (%)
HNSCCa	Affine	0.51 ± 0.23	93 ± 2
(n=11)	Affine + Demons	$0.43 \pm 0.16^{\dagger}$	$98 \pm 2^{\dagger}$
Thyroid	Affine	0.92 ± 0.45	91 ± 2
(n=6)	Affine + Demons	0.98 ± 0.42	$98 \pm 2^{\dagger}$

† Statistically significant compared to affine ($p<0.05$).

3. RESULTS

Seventeen patient tissue samples were registered according to the described methods, divided into two groups: HNSCCa (n=11) and thyroid (n=6). Table 1 shows the experimental results. Three representative patient results are shown in this manuscript. Figure 3 shows a glossal SCCa cancer margin with a needle-bored hole for TRE evaluation. Figure 4 shows the registered cancer margin for a papillary thyroid carcinoma sample, containing three needle-bored holes for TRE evaluation. Lastly, Figure 5 shows the registered cancer margin result of a tissue sample from oral SCCa without needle-bored holes, which represents how the registration pipeline would be put into experimental practice.

Affine registration alone of the representative tissue samples is insufficient to establish the cancer margin on the HSI, but the Demons-based method achieved successful alignment. For the HNSCCa group only, Demons registration produced better matched images (TRE of 0.43 ± 0.16 mm) with more consistent results between tissue samples compared to affine registration alone (TRE of 0.51 ± 0.23 mm). Moreover, the result for HNSCCa Demons registration was statistically significant (p=0.02) compared to affine, using a one-tailed, paired Student's t-test. In addition, for HNSCCa, the proposed deformable pipeline had a better image overlap compared to affine alone, DSC of 0.98 versus 0.93, which was also statistically significant ($p=5\times10^{-7}$).

The efficacy of both registration methods, affine and Demons, differed significantly for the thyroid group. On average the error for Demons registration of thyroid samples (TRE of 0.98 ± 0.42 mm) was comparable with affine registration alone (TRE of 0.92 ± 0.45 mm). However, the proposed deformable pipeline had a better image overlap for thyroid samples compared to affine alone, DSC of 0.98 versus 0.91, which was statistically significant ($p=9\times10^{-6}$). However, Demons registration did not show an advantage over affine registration for the thyroid samples.

Using a one-tailed, unpaired Student's t-test, the results of average error for HNSCCa Demons registration were compared to thyroid sample Demons registration, and the result was statistically significant (p=0.0007). This indicates that the registration of thyroid samples induces a substantially larger amount of error when compared to HNSCCa samples, most likely due to less structural integrity of the glandular thyroid tissue.

4. DISCUSSION

The potential of HSI and machine learning to provide diagnostic information about *ex-vivo* surgical specimens requires a consistent and reproducible technique for ground-truth cancer margin delineation for validation. This study aims solve this problem by describing a processing pipeline for deformable registration of the histological cancer margin to HSI of *ex-vivo* tissue samples for the intent of future use as validation for machine learning. The presented workflow uses affine and Demons-based registration that was evaluated on 17 patient tissue samples. This study investigated the ability to transform the cancer-normal margin from digitized histology to HS images of gross specimens.

Comparing deformable Demons registration to affine registration alone shows that the Demons-based method achieved successful image matching, while affine alone is insufficient to establish the gross-level cancer margin.

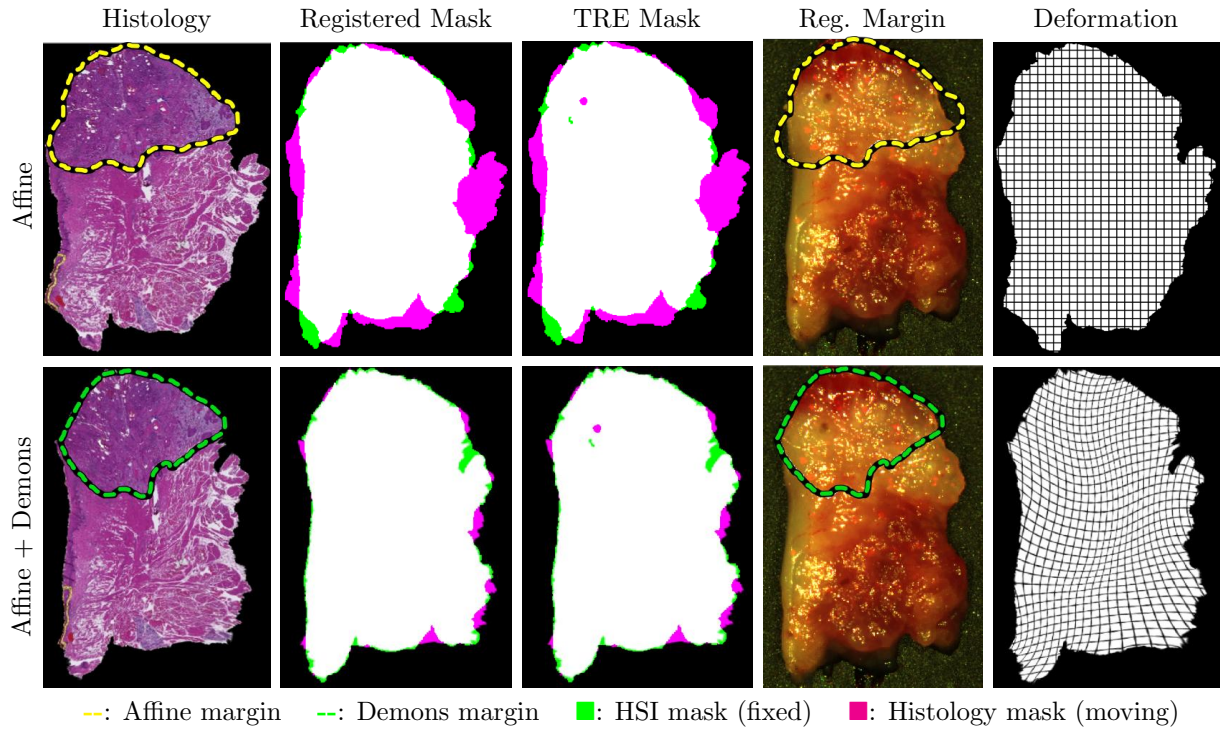

Figure 3. Results of affine and deformable Demons registration of the cancer-normal margin on glossal SCCa tissue sample with needle-bored holes. The cancer margin is outlined by a head & neck pathologist. The transformed margin from affine registration is outlined in yellow, and the margin from demons registration is outlined in green. The fixed HSI mask (green) and moving histology mask (magenta) overlap area is shown white. The TRE for this sample is evaluated using needle-bored holes shown on the masks in the center column. The deformation fields of the registration methods are shown on the right.

The efficacy of both registration methods, affine and Demons, differed to a statistically significant degree for the thyroid group. This indicates that registration of thyroid samples induces a substantially larger amount of error when compared to HNSCCa samples, most likely due to reduced structural integrity of the glandular and follicular composition of thyroid tissue.

The proposed method is necessary for HNSCCa samples to obtain the cancer margin and demonstrates the utility for future use. Tissue specimens from HNSCCa are usually difficult to classify visually with a high degree of certainty. However, the limited efficacy for thyroid tissue specimen registration is less concerning because the margin can be visibly identified by an individual educated in histology after confirming tissue composition and the true cancer boundary under histopathology. Therefore, it is possible to correct the deformable registration to align better on the cancer-margin for two reasons: normal follicular thyroid tissue has a dark-red appearance compared to the typical yellow-brown of carcinomas, and thyroid carcinomas tend have histologically visible capsules.

In summary, this work presents a promising processing method of deformable registration of the cancer margin from histological images onto HSI of gross specimens. Future research is needed to process more patient images with the workflow proposed and incorporate the method for validation of machine learning systems.

ACKNOWLEDGMENTS

This research is supported in part by NIH grants CA176684, CA156775 and CA204254, Georgia Cancer Coalition Distinguished Clinicians and Scientists Award, and the Developmental Funds from the Winship Cancer Institute of Emory University under award number P30CA138292. The authors would like to thank the surgical pathology

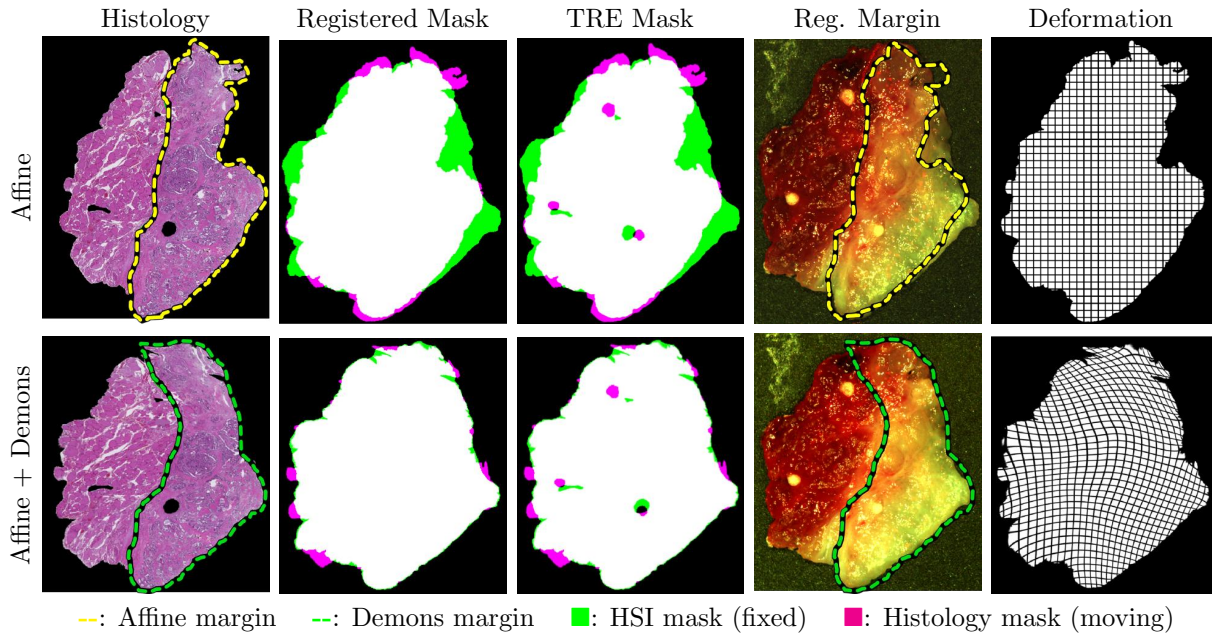

Figure 4. Results of affine and Demons registration of the cancer-normal margin on a thyroid tissue sample with needle-bored holes. The cancer margin is outlined by a head & neck pathologist. The transformed margin from affine registration is outlined in yellow, and the margin from demons registration is outlined in green. The fixed HSI mask (green) and moving histology mask (magenta) overlap area is shown white. The TRE for this sample is evaluated using needle-bored holes shown on the masks in the center column. The deformation fields of the registration methods are shown on the right.

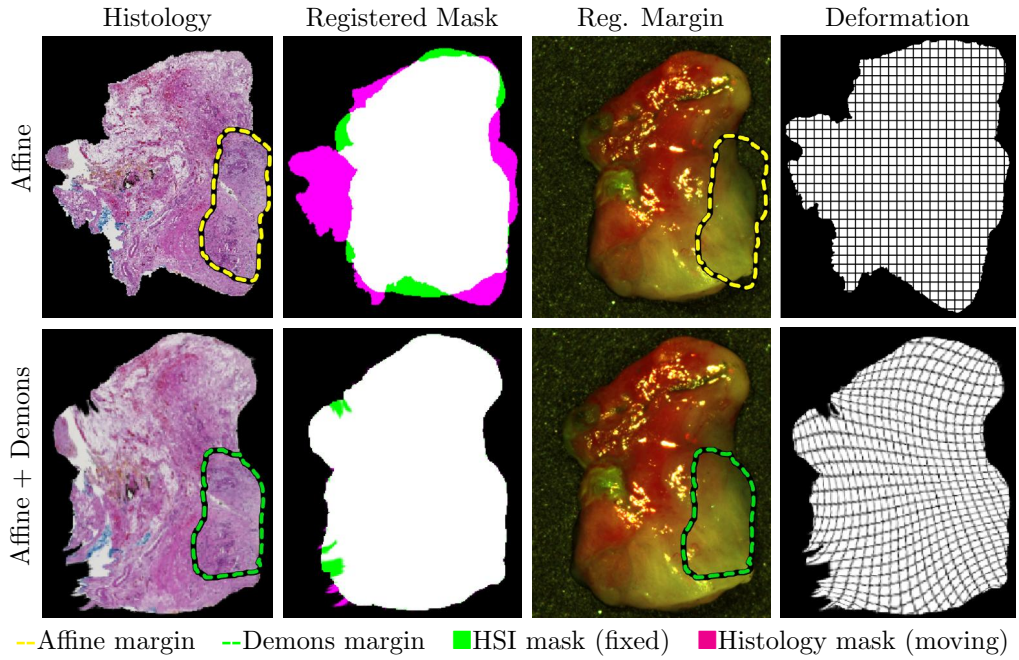

Figure 5. Results of affine and Demons registration of the cancer-normal margin on a SCCa sample from floor of mouth. The cancer margin is outlined by a head & neck pathologist. The transformed margin from affine registration is outlined in yellow, and the margin from demons registration is outlined in green. The fixed HSI mask (green) and moving histology mask (magenta) overlap area is shown white. The deformation fields of the registration methods are shown on the right.

team at Emory University Hospital Midtown including Andrew Balicki, Jacqueline Ernst, Tara Meade, Dana Uesry, and Mark Mainiero, for their help in collecting fresh tissue specimens.

REFERENCES

[1] Argiris, A., Karamouzis, M. V., Raben, D., and Ferris, R. L., "Head and neck cancer," *The Lancet.* **371**(9625), 1695 – 1709 (2008).

[2] Joseph, L. J., Goodman, M., Higgins, K., Pilai, R., Ramalingam, S. S., Magliocca, K., Patel, M. R., El-Deiry, M., Wadsworth, J. T., Owonikoko, T. K., Beitler, J. J., Khuri, F. R., Shin, D. M., and Saba, N. F., "Racial disparities in squamous cell carcinoma of the oral tongue among women: A SEER data analysis," *Oral Oncology.* **51**(6), 586–592 (2015).

[3] Meier, J. D., Oliver, D. A., and Varvares, M. A., "Surgical margin determination in head and neck oncology: Current clinical practice. The results of an international american head and neck society member survey," *Head & Neck.* **27**(11), 952–958 (2005).

[4] Hinni, M. L., Ferlito, A., Brandwein-Gensler, M. S., Takes, R. P., Silver, C. E., Westra, W. H., Seethala, R. R., Rodrigo, J. P., Corry, J., Bradford, C. R., Hunt, J. L., Strojan, P., Devaney, K. O., Gnepp, D. R., Hartl, D. M., Kowalski, L. P., Rinaldo, A., and Barnes, L., "Surgical margins in head and neck cancer: A contemporary review," *Head & Neck.* **35**(9), 1362–1370 (2013).

[5] Novis, D. A. and Zarbo, R. J., "Interinstitutional comparison of frozen section turnaround time. A College of American Pathologists Q-Probes study of 32868 frozen sections in 700 hospitals," *Arch. Pathol. Lab. Med.* **121**, 559–567 (Jun 1997).

[6] Chen, T. Y., Emrich, J. L., and Driscoll, D. L., "The clinical significance of pathological findings in surgically resected margins of the primary tumor in head and neck carcinoma," *International Journal of Radiation Oncology.* **13**, 883–837 (June 1987).

[7] Loree, T. R. and Strong, E. W., "Significance of positive margins in oral cavity squamous carcinoma," *American Journal of Surgery.* **160**, 410–414 (Oct 1990).

[8] Sutton, D. N., Brown, J. S., Rogers, S. N., Vaughan, E. D., and Woolgar, J. A., "The prognostic implications of the surgical margin in oral squamous cell carcinoma," *Intl. J. Oral and Maxillofacial Surgery.* **32**, 30–34 (Feb 2003).

[9] Rathod, S., Livergant, J., Klein, J., Witterick, I., and Ringash, J., "A systematic review of quality of life in head and neck cancer treated with surgery with or without adjuvant treatment," *Intl. J. Oral and Maxillofacial Surgery* **51**, 888–900 (Oct 2015).

[10] Pimenta Amaral, T. M., Da Silva Freire, A. R., Carvalho, A. L., Pinto, C. A., and P, K. L., "Predictive factors of occult metastasis and prognosis of clinical stages I and II squamous cell carcinoma of the tongue and floor of the mouth," *Oral Oncology* **40**, 780–786 (Sep 2004).

[11] Garzino-Demo, P., Dell'Acqua, A., Dalmasso, P., Fasolis, M., Maggiore, G. M. L. T., Ramieri, G., Berrone, S., Rampino, M., and Schena, M., "Clinicopathological parameters and outcome of 245 patients operated for oral squamous cell carcinoma," *Journal of Cranio-Maxillofacial Surgery.* **34**(6), 344–350 (2006).

[12] Rogers, W., Ryack, B., and Moeller, G., "Computer-aided medical diagnosis: Literature review," *International Journal of Bio-Medical Computing.* **10**(4), 267 – 289 (1979).

[13] Halicek, M., Lu, G., Little, J. V., Wang, X., Patel, M., Griffith, C. C., El-Deiry, M. W., Chen, A. Y., and Fei, B., "Deep convolutional neural networks for classifying head and neck cancer using hyperspectral imaging," *Journal of Biomedical Optics.* **22**(6), 060503 (2017).

[14] Fei, B., Lu, G., Wang, X., Zhang, H., Little, J. V., Patel, M. R., Griffith, C. C., El-Diery, M. W., and Chen, A. Y., "Label-free reflectance hyperspectral imaging for tumor margin assessment: a pilot study on surgical specimens of cancer patients," *Journal of Biomedical Optics.* **22**(8) (2017).

[15] Lu, G., Little, J. V., Wang, X., Zhang, H., Patel, M., Griffith, C. C., El-Deiry, M., Chen, A. Y., and Fei, B., "Detection of head and neck cancer in surgical specimens using quantitative hyperspectral imaging," *Clinical Cancer Research.* (2017).

[16] Akbari, H., Halig, L. V., Zhang, H., Wang, D., Chen, Z. G., and Fei, B., "Detection of cancer metastasis using a novel macroscopic hyperspectral method," *Proc. SPIE.* **8317**, 831711–1–7 (2012).

[17] Fitzpatrick, J. M. and West, J. B., "The distribution of target registration error in rigid-body point-based registration," *IEEE Transactions on Medical Imaging* **20**, 917–927 (Sept 2001).

[18] Hill, D. L. G., Batchelor, P. G., Holden, M., and Hawkes, D. J., "Medical image registration," *Physics in Medicine & Biology.* **46**(3), R1 (2001).

[19] Crum, W. R., Hartkens, T., and Hill, D. L. G., "Non-rigid image registration: theory and practice," *The British Journal of Radiology.* **77**(2), S140–S153 (2004). PMID: 15677356.

[20] Lu, G., Halig, L., Wang, D., Chen, Z. G., and Fei, B., "Hyperspectral imaging for cancer surgical margin delineation: registration of hyperspectral and histological images," *Proc. SPIE.* **9036**, 90360S–1–8 (2014).

[21] Thirion, J.-P., "Image matching as a diffusion process: an analogy with maxwell's demons," *Medical image analysis.* **2 3**, 243–60 (1998).

[22] Horn, B. K. P. and Schunck, B. G., "Determining optical flow," *Artif. Intell.* **17**, 185–203 (Aug. 1981).